J Oceanogr (2014) 70:435–445
DOI 10.1007/s10872-014-0244-6

ORIGINAL ARTICLE

Biogeochemical responses associated with the passage of a cyclonic eddy based on shipboard observations in the western North Pacific

Chiho Sukigara · Toshio Suga · Katsuya Toyama · Eitarou Oka

Received: 18 March 2014 / Revised: 25 August 2014 / Accepted: 31 August 2014 / Published online: 20 September 2014

Abstract A shipboard high-resolution hydrographic survey in the subtropical region of the western North Pacific conducted from October to November 2008 detected part of a cyclonic eddy around 30°N, 145°E. This eddy had propagated westward in the region south of the Kuroshio extension for at least 6 months as a wavelike disturbance. Within this eddy, isopycnals shallowed between a depth of 600 m and just below the surface mixed layer. In addition, maximal dissolved oxygen concentrations were observed in the subsurface layer between depths of 50 and 100 m. Nitrate was depleted within this subsurface maximal oxygen layer. These results suggest that nutrients in the deeper layers were supplied into the euphotic layer as a result of the uplift of isopycnals in the eddy, fueling the photosynthesis of phytoplankton in the subsurface and emitting an excess of oxygen due to new production. Compared with the outside of the eddy, the enhancement of oxygen and the decrease of nitrate in the center of the eddy were estimated to be 2.7 mol O_2 m^{-2} and 0.22 mol N m^{-2}, respectively. The primary productivity calculated using the eddy transition speed of 5.1 km day^{-1} was 548 mg C m^{-2} day^{-1} at the center of the eddy. The enhanced primary productivity due to the passage of the eddy is likely to have an important role in the ecosystem and on material cycling in the subtropical region.

Keywords Mesoscale process · Physical–biological process · Cyclonic eddy · Primary productivity · Nutrient supply

C. Sukigara (✉)
Hydrospheric Atmospheric Research Center, Nagoya University, Nagoya, Japan
e-mail: suki@hyarc.nagoya-u.ac.jp

T. Suga
Department of Geophysics, Graduate School of Science, Tohoku University, Sendai, Japan

T. Suga
Research Institute for Global Change, Japan Agency of Marine-Earth Science and Technology, Yokosuka, Japan

K. Toyama
The Program in Atmospheric and Oceanic Sciences, Princeton University, Princeton, NJ, USA

E. Oka
Atmosphere and Ocean Research Institute, The University of Tokyo, Chiba, Japan

1 Introduction

Mesoscale perturbations are ubiquitous in the ocean, and enrich the spatial and temporal variability of the oceanic structure. They also influence the distribution of materials, biomass, and biogeochemical processes through variations in the physical conditions. McGillicuddy and Robinson (1997) described the mesoscale dynamic processes that operated during nutrient cycling in the Sargasso Sea. Their conceptual model explained that cyclonic eddies and mode-water eddies raise the density surface toward the surface, while anticyclonic eddies push the density surface down. When deep water rich in nutrients is injected into the euphotic zone by the upwelling created by eddies, phytoplankton can use the nutrients, and the biomass and the primary production is enhanced. On this basis, nitrate fluxes in the Sargasso Sea associated with eddies were estimated to be 0.35 ± 0.10 mol N m^{-2} $year^{-1}$ using a regional, eddy-resolving, coupled physical–biological model. Furthermore, the nitrate flux in the Sargasso Sea was estimated to be 0.19 ± 0.10 mol N m^{-2} $year^{-1}$ using

a statistical model based on satellite-derived sea surface height (SSH) anomalies and the mean relationship between density and nitrate concentration (McGillicuddy et al. 1998). These estimated values of the nitrate flux by eddies were larger than those of nitrogen supply by winter convection (0.09 ± 0.04 to 0.17 ± 0.05 mol N m^{-2} $year^{-1}$; Michaels et al. 1994), diapycnic diffusion (0.05 ± 0.01 mol N m^{-2} $year^{-1}$; Lewis et al. 1986), nitrogen fixation (0.07 mol N m^{-2} $year^{-1}$; Gruber and Sarmiento 1997), or atmospheric deposition (0.03 mol N m^{-2} $year^{-1}$; Knap et al. 1986). However, Oschlies (2002) reported that typical values of the simulated eddy-induced nitrate supply near the Sargasso Sea were only 0.05 mol N m^{-2} $year^{-1}$, based on an eddy-resolving coupled ecosystem–circulation model for the North Atlantic. Martin and Pondaven (2003) suggested that the vertical nitrate fluxes due to eddy pumping based on altimetry were likely to be overestimated, due to the spatial bias of eddy location and the low efficiency of nutrient uptake by phytoplankton in response to eddy pumping. Although model estimates of the nutrient fluxes associated with eddies vary widely, these results strongly suggested that cyclonic eddies and mode-water eddies might play a substantial role in nutrient supply to the oligotrophic subtropical surface layer. Therefore, field observations are required to verify the impact of eddies on biological processes.

Interdisciplinary field studies in subtropical regions (e.g., E-Flux programs in the North Pacific (Benitez-Nelson et al. 2007) or the EDDIES program in the North Atlantic (McGillicuddy et al. 2007) have been conducted to investigate eddy-induced perturbations of the physical and biological environment, the response of the plankton community to eddies, and the resulting impacts on biogeochemical cycling and export (Benitez-Nelson and McGillicuddy 2008). These programs have revealed that biological and biogeochemical responses within eddies differ due to variations in the eddy magnitude, and the timing and duration of nutrient inputs caused by differences in the eddy formation process, intensity, age and movement. For example, Cyclone *Opal* observed in the E-Flux program, which was a strong eddy formed by a combination of strong winds and topography in the lee of the Hawaiian Islands, involved an eddy-induced nitrate injection (Mahaffey et al. 2008) and an extraordinary diatom bloom (Bibby et al. 2008; Brown et al. 2008). These strong biological signals were suggested to have resulted from large isopycnal displacements of over 100 m at the eddy core that lasted for about one month (Dickey et al. 2008; Nencioli et al. 2008). Furthermore, this eddy was suggested to have been continuously entraining nutrients from the deeper layer to the euphotic zone within the moving trail of the eddy (Nencioli et al. 2008). In another case, a mode water eddy in the Sargasso Sea was observed with an enhanced nutrient injection and large diatom biomass (Bibby et al. 2008; Ewart et al. 2008), despite the advanced age of the eddy. This was suggested to be the result of a continuous upwelling of nutrients by eddy–wind interactions with strong mixing at the core of the eddy (Greenan 2008). The nutrient injection processes and the associated biological responses intricately vary depending on the eddy features, the surrounding circumstances, and the ecosystem in the eddy (Martin and Pondaven 2003; Siegel et al. 2011). High-resolution and three-dimensional observations are required to investigate the impacts of eddies on the biogeochemical processes.

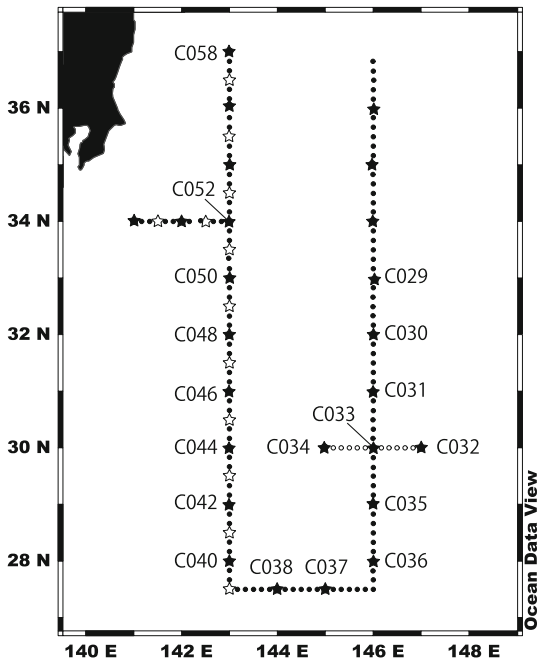

Fig. 1 Location of $CTDO_2$ stations with water sampling (*closed stars*), $CTDO_2$ stations without water sampling (*open stars*), XCTD stations (*closed circles*), and XBT stations (*open circles*) for the KH-08-3 cruise leg 2 from 22 October to 4 November 2008

In this study, we focused on an eddy in the subtropical region several hundred kilometers south of the Kuroshio extension (KE) in the western North Pacific. This area is in the path of westward propagating cyclonic and/or anticyclonic eddies (Ebuchi and Hanawa 2000, 2001). Few studies have reported on the physical structure of eddies and particularly their influence on biological processes in this region. Our aim was to analyze the relationships among the physical structures, eddy movement, and biogeochemical responses.

2 Observation

A high-resolution hydrographic survey was conducted from 9 October to 7 November 2008 in the western North Pacific southeast of Japan during the KH-08-3 cruise leg 2

of R/V *Hakuho-Maru*, targeting the mesoscale distribution of the North Pacific subtropical mode water (Oka et al. 2011). Two meridional lines at 143°E and 146°E and three shorter zonal lines at 27.5°N, 30°N, and 34°N were surveyed using a conductivity–temperature–depth–oxygen profiler ($CTDO_2$, Model9-plus; Sea-Bird Electronics Inc., Bellevue, WA, USA) at intervals of 30′ or 1° in latitude/longitude, and an expendable conductivity–temperature–depth profiler (XCTD; Tsurumi Seiki Co. Ltd., Yokohama, Japan) or an expendable bathythermograph (XBT, Tsurumi Seiki Co. Ltd.) at 10′ intervals (Fig. 1). A salinity profile at each XBT station was estimated using the observed temperature and temperature–salinity relations at nearby $CTDO_2$ stations (Oka et al. 2011). Water samples for salinity, nutrient, dissolved oxygen (DO), and chlorophyll *a* (Chl *a*) measurements were collected at 1° intervals at $CTDO_2$ stations.

Salinity and oxygen sensors in the $CTDO_2$ system were calibrated using water samples. Salinity and DO in sampled water were measured using an onboard Portasal 8410 salinometer (Guideline Instruments, Smiths Falls, ON, Canada) and titration unit (MPT Titrino 798; Metrohm Shibata, Tokyo, Japan), respectively. The saturation concentration of DO was computed for each layer from the observed potential temperature and salinity (Weiss 1981). The DO saturation ratio (DO%) was calculated by dividing the observed DO by the saturation concentration of DO. Nutrient (nitrate: NO_3^-, nitrite: NO_2^-, phosphate: PO_4^- and dissolved silicate: SiO_2) concentration was measured with a TRACCS 2000 autoanalyzer (Bran+Luebbe, Norderstedt, Germany) after the cruise. The nitrate was reduced to nitrite using a cadmium–copper column and the concentration was determined by absorption spectrometry of an azo dye coupled with *N*-(1-naphthyl)-ethylenediamine dihydrochloride. The concentration of nitrite was determined by absorption spectrometry of an azo dye (Armstrong et al. 1967). The concentrations of phosphate and dissolved silicate were determined by absorption spectrometry of heteropoly-molybdenum blue (Murphy and Riley 1961; Koroleff 1983). Nutrient samples were kept in a freezer for measurement. The vertical resolution of nutrients was 10 m in the top 200-m layer and 100 m in the 200–600-m layer. Chl *a* samples were measured onboard using a fluorometer (10-AU; Turner Designs, Sunnyvale, CA, USA). The vertical resolution of chlorophyll was 10 m in the top 160-m layer and 20 m in the 160–200-m layer. The light environment of the water column was obtained using a photosynthetically active radiation (PAR) sensor (QSP-2200; Biospherical Instruments Inc., San Diego, CA, USA). Current velocity and direction during the entire cruise were measured by a ship-mounted acoustic Doppler current profiler (ADCP, Ocean Surveyor 38 kHz; Teledyne RD Instruments Inc., Poway, CA, USA). The profile depths ranged from 32 to 1296 m, with a vertical resolution of 16 m.

The spatial distribution of SSH and its anomalies in the observation period was based on delayed-time maps of absolute dynamic topography and sea level anomalies produced by merging the data from two satellites, Jason-1 and Envisat, at the AVISO (http://www.aviso.altimetry.fr/en/home.html; Ducet et al. 2000). The spatial and temporal resolutions were 0.25° in latitude and longitude and every 7 days.

3 Results

In this study, we focused on the subtropical area south of the KE, whose southern flank was located at 32.5°N on the 146°E line and 34°N on the 143°E line. Vertical sections of the hydrographic and biogeochemical data for each transect are shown in Fig. 2. On the 146°E line, isopleths of potential density (isopycnals) below 200 m depth shallowed sharply from 32°N to 33°N in association with KE (Fig. 2a).

A distinct uplift of the isopycnals from a depth of 600 m ($26.6\sigma_\theta$) to a seasonal pycnocline (up to 50 m and $24.0\sigma_\theta$) appeared around 30°N on the 146°E line. The largest uplift on the 146°E line was observed at 30.3°N, and the $25.2\sigma_\theta$ isopycnal reached 130 m. This was substantially shallower than in the vicinity of the same transect; the depth of the $25.2\sigma_\theta$ isopycnal was 200 m at 29°N and 250 m at 32°N. On the 30°N line, isopycnals denser than $25.0\sigma_\theta$ tended to shallow toward the west. The depth of the $25.2\sigma_\theta$ isopycnal reached a depth of 100 m at 145°E and was the shallowest of all stations (Figs. 2a, 3a). An obvious heaving of the $25.2\sigma_\theta$ isopycnal also appeared at 29.2°N on the 143°E line. The magnitude and width of uplift was smaller than at the 146°E line. The spatial distribution of SSH in the observation period showed a moderate depression centered at 29°N and 145°E (Fig. 4). The position of the depression in the SSH roughly coincided with the uplift of the isopycnals at 146° and 143°E.

The downward decrease in DO below a depth of approximately 200 m associated with the increase of potential density was caused by oxygen consumption during respiration by organisms and remineralization by bacteria. Exceptionally high DO and DO% layers appeared from 150 to 400 m at 143°E and from 400 to 600 m at 145°E on the 27.5°N transect (Figs. 2b, c, 3b, c). The former resulted from subtropical mode water, which is depicted in the vertical distribution of potential density and potential vorticity (Oka et al. 2011). The latter was associated with North Pacific central mode water contained in a subsurface mesoscale eddy (Oka et al. 2009). Supersaturations of DO% were found in the layer from 50 to 100 m

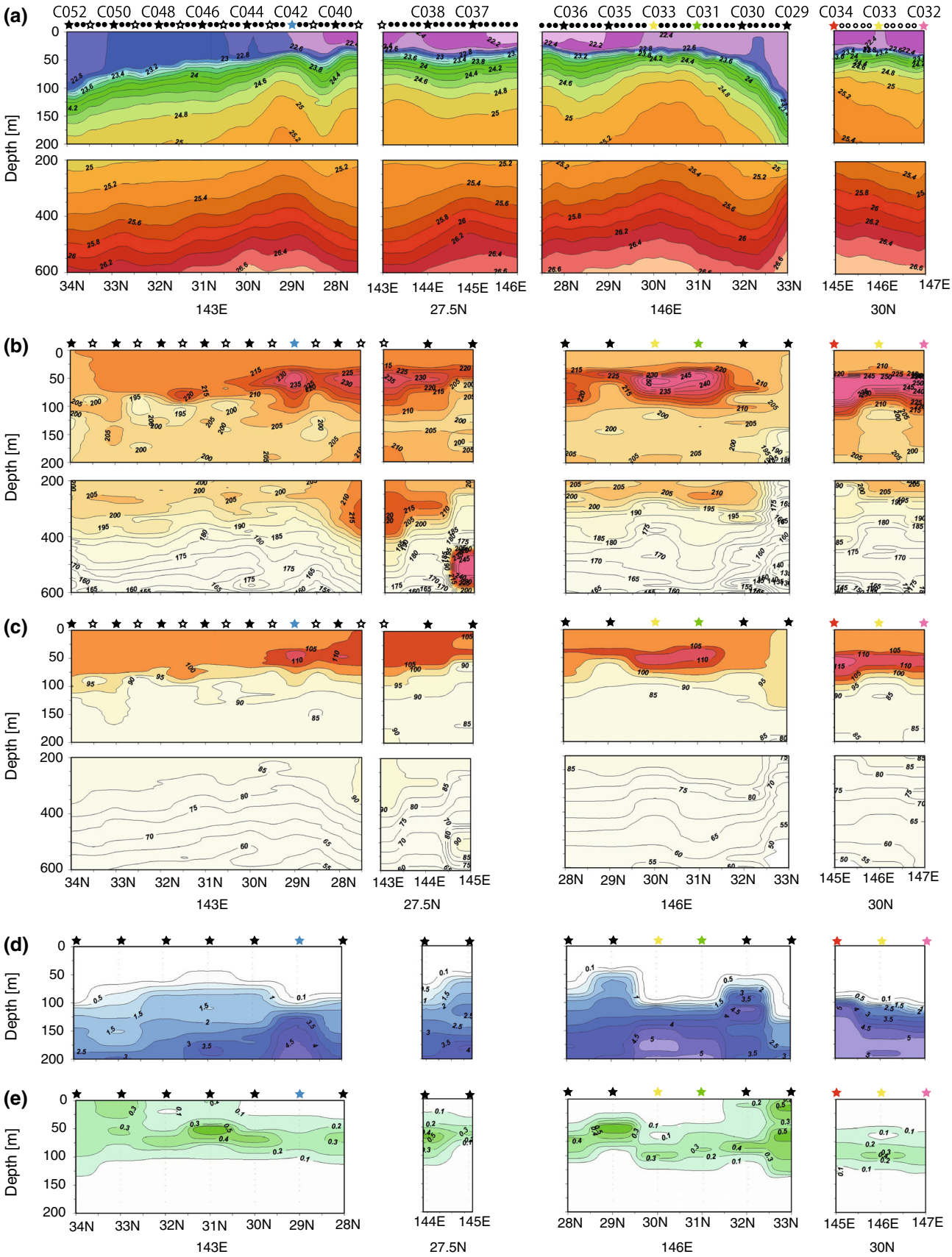
(a)
C052 C050 C048 C046 C044 C042 C040
C038 C037
C036 C035 C033 C031 C030 C029
C034 C033 C032
Depth [m]
34N 33N 32N 31N 30N 29N 28N
143E
143E 144E 145E 146E
27.5N
28N 29N 30N 31N 32N 33N
146E
145E 146E 147E
30N
(b)
(c)
(d)
(e)

◀**Fig. 2** Spatial distributions of **a** potential density (σ_θ) (kg m^{-3}), **b** dissolved oxygen (DO) concentration (μmol kg^{-1}), **c** DO saturation ratio (%), **d** nitrate concentration (μmol L^{-1}), and **e** chlorophyll *a* (μg L^{-1}) in the hydrographic sections of the KH-08-3 cruise leg 2. *Closed stars, open stars, closed circles*, and *open circles* on the figures indicate CTDO$_2$ stations with water sampling, CTDO$_2$ stations without water sampling, XCTD stations, and XBT stations, respectively. *Colored stars* indicate the CTDO$_2$ stations with water sampling in the eddy

in the southern stations (Figs. 2c, 3c). Significant supersaturated subsurface oxygen maximum (SOM) layers were observed at five stations, C031 (31°N, 146°E), C032 (30°N, 146°E), C033 (30°N, 147°E), C034 (30°N, 145°E), and C042 (29°N, 143°E), where isopycnals were lifted as described above (Fig. 2c). SOM layers are often observed and extend from the bottom of the surface mixed layer to the bottom of the euphotic zone, where light intensity falls to 1 % of that at the surface (Shulenberger and Reid 1981; Hayward 1994).

The depth of the euphotic layer observed using the PAR sensor in this cruise was estimated to be between 50 and 70 m from the surface. When the mixed layer depth was defined as the depth at which the difference in temperature from the 5 m depth was 0.1 °C, the thickness of the mixed layer on the south of 32°N was at a < 50 m depth from the surface. The nitrate concentration within the euphotic layer, whose depth was deeper than the depth of the mixed layer, in the observed subtropical region was low (<0.1 μmol L^{-1}) because of its utilization by phytoplankton in photosynthesis and the poor supply from deeper layers. Therefore, it was considered reasonable that the depth of the top of the nitracline almost corresponded to the depth of the bottom of euphotic layer (Figs. 2d, 3d). However, the nitracline deepened to a depth of around 100 m at the five stations (C031, C032, C033, C034, and C042) where the isopycnals were uplifted. The low nitrate concentration in these stations was found not only in the euphotic zone, but also below the euphotic zone (80–100 m) and increased significantly from 80 to 130 m. The low concentration of nitrate and the relatively high concentration of DO below the euphotic zone in these stations suggested the following scenario: The water with rich nitrate and low DO below the euphotic zone was uplifted into the euphotic zone, nitrate in the water was utilized for new production by phytoplankton, through which excess oxygen emitted, and then the water with low nitrate and high DO sunk below the euphotic zone. The spatial variations of phosphate and silicate concentrations were similar to that of nitrate. The low concentrations of silicate at the five stations (C031, C032, C033, C034, and C042) suggest the increase of diatoms, as observed in the mode-water eddy in North Atlantic and the cyclonic eddy in North Pacific (Benitez-Nelson et al. 2007; McGillicuddy et al. 2007; Bibby et al. 2008; Brown et al. 2008).

Vertical peaks of Chl *a* often appeared in the subsurface in the oligotrophic subtropical region, which is referred to

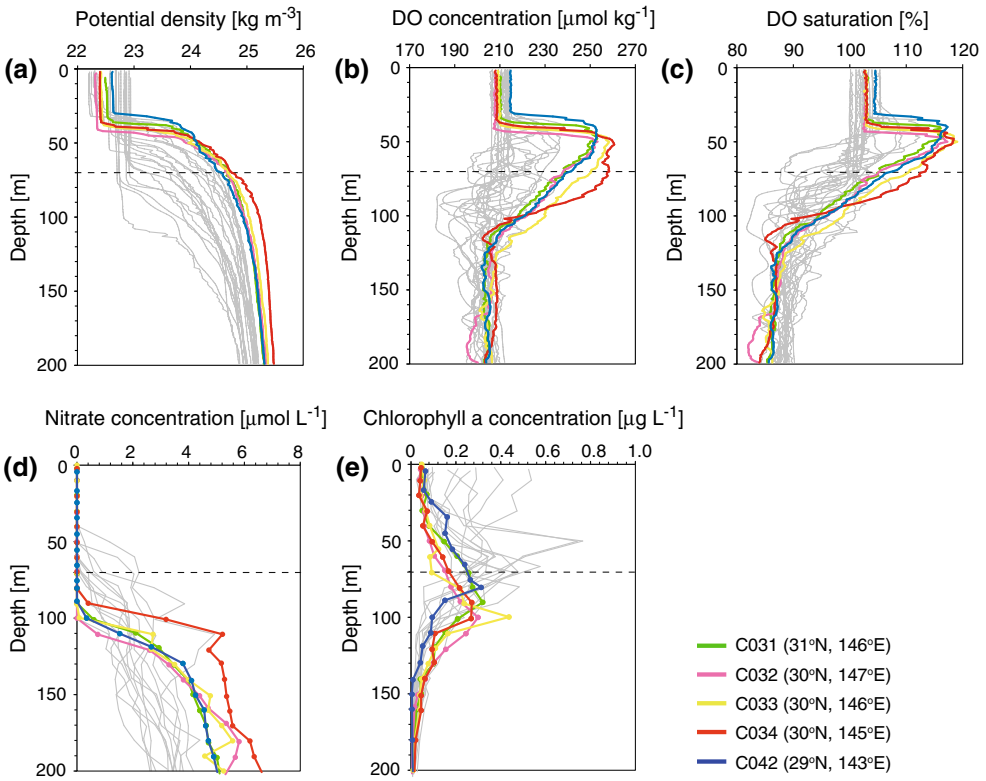

Fig. 3 Vertical profiles of **a** potential density (kg m^{-3}), **b** dissolved oxygen (DO) concentration (μmol kg^{-1}), **c** DO saturation (%), **d** nitrate concentration (μmol L^{-1}), and **e** chlorophyll *a* concentration (μg L^{-1}). *Colored* and *gray lines* are the profiles for stations inside and outside the eddy, respectively. *Broken lines* at the 70 m depth indicate the bottom of the euphotic zone

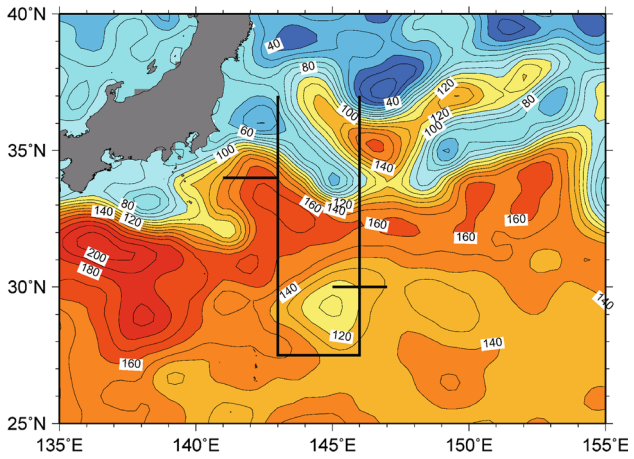

Fig. 4 The altimetric sea surface height map southeast of Japan on 22 October 2008. *Thick black lines* indicate the hydrographic sections of the KH-08-3 cruise leg 2

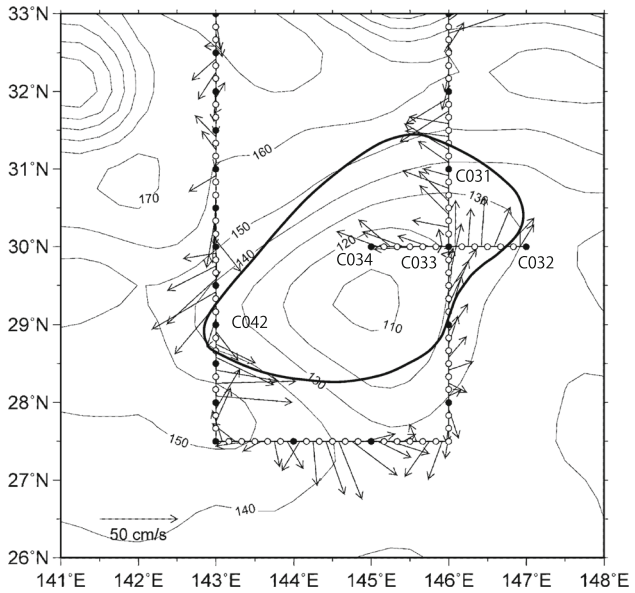

Fig. 5 ADCP velocity (*arrows*) at 50-m depth measured during the KH-08-3 cruise leg 2. The *closed* (*open*) *circles* indicate the locations where $CTDO_2$ (XCTD and XBT) observations were made. *Thin contours* denote altimetric sea surface height on 22 October 2008. *Thick contour* represents a geopotential anomaly contour of 1.85 dynamic meters relative to 794 dbar, the deepest common level of the hydrographic data

as the deep Chl *a* maximum (DCM; Cullen 1982). High Chl *a* concentrations (>0.5 μg L^{-1}) were observed around a depth of 60 m at 29° and 33°N on the 146°E line, and 31°N on the 143°E line (Fig. 2e). However, the DCM at the stations with uplifted isopycnals (C031, C032, C033, C034, and C042) was deeper (≈100 m) than at the other stations (Figs. 2e, 3e). The Chl *a* concentrations in the deeper DCM layer were about 0.3 μg L^{-1} and lower than those in other stations.

4 Discussion

4.1 A mesoscale cyclonic eddy and biochemical responses to the passage of the eddy

Uplifts of isopycnals around 30°N (Fig. 2a) appeared inside the low SSH region (Fig. 4). Therefore, a cyclonic eddy was suggested to have had an influence on the structure of the water mass and the biogeochemical processes in this area. The ADCP velocity at 50 m depth obtained along the observation lines (Fig. 5) revealed a velocity field dominated by the presence of the cyclonic flow of the eddy. The direction of the current was westward between 32°N and 30°N, northeastward between 30°N and 29°N along the 146°E line, and northward between 146°E and 147°E along the 30°N line. These directions showed that the region from 29°N to 32°N on the 146°E line and from 145°E to 147°E on the 30°N line was located within the eastern half of the cyclonic eddy. Station C034 at 30°N, 145°E was probably closest to the core of the eddy among the CTD stations along the 146°E line and the 30°N line. Current directions around station C032 at 30°N, 147°E indicated that the eddy had already passed this station. Along the 143°E line, the direction of the current was southwestward between 29°N and 30°N, and eastward between 28°N and 29°N. Current speeds reached 50 cm s^{-1} for the southeastward and westward currents, but were as low as 10 cm s^{-1} at station C042 (29°N, 143°E). The region from 28°N to 30°N on the 143°E line was thought to be occupied by the western half of the eddy.

We also drew contours of geopotential anomaly computed from the hydrographic data with the ADCP velocity, following Martin and Richards (2001) (Fig. 5). The contour of 1.85 m at the sea surface relative to 794 dbar (the deepest common level of the hydrographic data) includes the four CTD stations (C031, C033, C034, and C042) with the biogeochemical response, and neighbors the remaining station (C032) to its immediate east. Therefore, this contour is expected to outline the cyclonic eddy.

The shape of the eddy, as suggested by the distribution of current velocity and SSH during our observation period, was an irregular circle with a minor axis 300 km in length that extended in the northwest and southeast directions, and a major axis 500 km in length that extended in the northeast and southwest directions (Fig. 4). From February to April 2008, the eddy approached the meandering KE at around 29°N, 154°E and its intensity increased, as illustrated by the depression of SSH (Fig. 6). After late April 2008, the eddy departed from the KE, propagated westward with the same intensity, reached the area around 29°N,

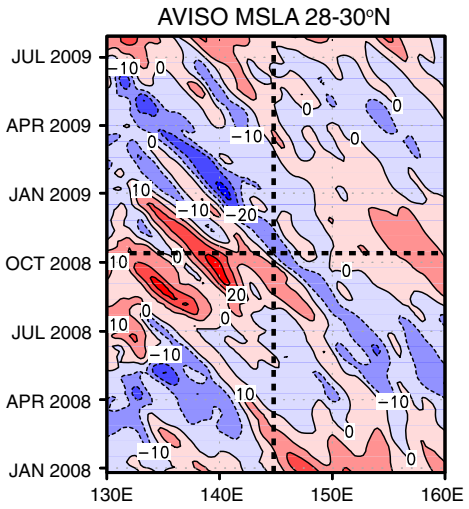

Fig. 6 Time series of sea surface height anomalies along the zonal band of 28–30°N. *Vertical* and *horizontal broken lines* show the position and the time of the observation, respectively

145°E (Oka et al. 2011) in October 2008, and was finally absorbed by the Kuroshio at around 29°N, 133°E in May 2009. The speed of propagation of the eddy from April 2008 to May 2009 was estimated as 5.8 km day^{-1} (6.7 cm s^{-1}). The transit speed of the center of the eddy from 8 October to 5 November 2008, including the ship observation period, was calculated 5.1 km day^{-1} (5.9 cm s^{-1}) based on the satellite altimetry-derived eddy trajectory data set (http://cioss.coas.oregonstate.edu/eddies/) produced by Chelton et al. (2011). The data set indicated that the origin of this eddy could be dated back to mid-April 2007 at around 27.2°N, 167.6°E. The age of the eddy since generation at the time of observation was 18 months, and 6 months had passed since the eddy had separated from the KE. Ebuchi and Hanawa (2000) reported typical shapes, behaviors, and spatial distribution of mesoscale cyclonic and anticyclonic eddies in the Kuroshio recirculation region. They reported that typical eddies in this region are circular in shape with a diameter of about 500 km, and the surface velocity, SSH anomaly, and phase speed of westward propagation were 15–20 cm s^{-1}, 15 cm, and 7 cm s^{-1}, respectively. The eddies were considered to be successive wavelike disturbances rather than solitary eddies.

This study focused on five CTD stations (C031, C032, C033, C034, and C042) that were located in the cyclonic eddy. These stations had common characteristics, such as uplifted isopycnals in a shallow layer, large SOM, a deep and steep nitracline, and a deep DCM compared with locations outside the eddy (Figs. 3, 7). Because the temperature–salinity relationship inside the eddy was similar to that outside the eddy (Fig. 8), the water in the eddy was considered to have originated from south of the KE. These observations suggested that the uplift of isopycnals by the eddy injected nutrients from the deeper layer to a nutrient-depleted euphotic zone, enhanced the primary productivity of phytoplankton through nutrients from the disphotic zone, and emitted surplus oxygen due to photosynthesis in the area where the eddy passed (McGillicuddy et al. 1998; Nencioli et al. 2008).

Figures 3 and 7 show that the five stations each had different features in their vertical structure and biological parameters. The potential density below 50 m depth at station C034 was higher than at the other stations, which suggests that station C034 was the closest station to the eddy center. Because the depth of the euphotic zone was 70 m, the density at the bottom of the euphotic zone was 24.8σ_θ at station C034. Compared with the potential density profiles at the stations outside the eddy, this isopycnal surface was presumably uplifted 30 m from a deeper layer. Of all the stations in the eddy, station C034 also had the highest level of DO in the SOM layer. The nitracline was shallower than at other stations and was located just below the euphotic zone. The high new productivity would have occurred at station C034.

Station C033 had the second highest potential density at the bottom of the euphotic zone and the second largest SOM layer. Of particular note was that the level of DO from 100 to 130 m depth at this station was relatively high. Nitrate was depleted down to a depth of 100 m and the nitracline was the deepest among the five stations. The distance from the eddy core to station C033 was larger than that at station C034. These features, including the large SOM layer and deep nitracline, suggest that the isopleths at station C033 sank to a deeper layer due to the biological responses, after they were uplifted into the euphotic zone, as occurred at station C034. Furthermore, these biological responses below the euphotic zone at station C033 suggested that the sinking of the water mass happened within a few weeks, which was estimated by the average transition speed of the eddy (5.1 km day^{-1}) and the distance between stations C034 and C033 (about 100 km). If a long time had passed after the sinking of the isopleths, DO and nitrate anomalies should have been dissipated by diffusion and advection or offset by respiration and remineralization. Vertical profiles of potential density, DO, and nutrients at stations C031, C032, and C042, which were located at the edge of the eddy, were similar to each other.

4.2 Quantitative estimation of the biochemical responses to the passage of the eddy

The estimation of a nutrient flux, which was uplifted from the deeper layer to the euphotic zone by the passage of the cyclonic eddy, is important for understanding the biological productivity and material cycling in this region. In

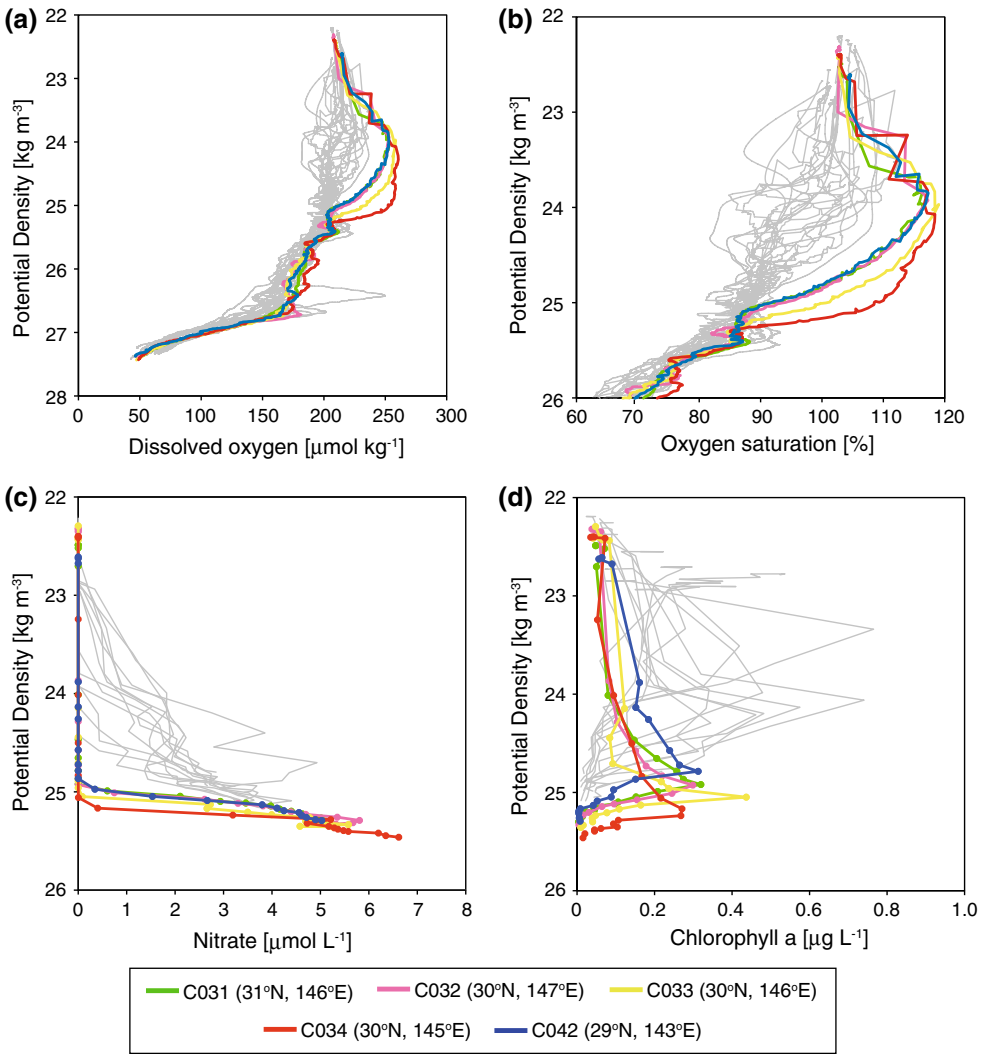

Fig. 7 Vertical potential density profiles of **a** dissolved oxygen (DO) concentration (µmol kg^{-1}), **b** DO saturation (%), **c** nitrate concentration (µmol L^{-1}), and **d** chlorophyll *a* concentration (µg L^{-1}). *Colored* and *gray lines* are the profiles for stations inside and outside the eddy, respectively

theory, the level of new primary production should be reflected by increases in organic carbon, DO, and the decrease of nutrients. However, these signals dissipate with time due to physical processes such as advection and diffusion, and biological processes such as grazing, particle sinking, and decomposition. Therefore, sparse and traditional snapshot observations from research vessels cannot collect sufficient data for estimating a nutrient flux and the subsequent primary production influenced by the eddy. Here, we attempted to make a quantitative estimation of the biological impact of the passage of the eddy by comparing biogeochemical parameters inside and outside the eddy using the high-resolution hydrographic survey data set.

To define the vertical variation of DO at a station outside the eddy, averaged DO concentrations for every $0.1\sigma_\theta$ were estimated at six stations (C030, C035, C036, C040, C041, and C044) located outside the eddy. The increased DO associated with the eddy passage was estimated from the difference between each value in the eddy and the averaged values outside of the eddy at the same density. This estimation was based on the hypothesis that the eddy did not transport water, but only propagated the uplift of isopycnals westward. Table 1 shows the integrated differences in the DO from the seasonal thermocline ($23.2–23.7\sigma_\theta$) to $25.2\sigma_\theta$, where large SOM layers existed (Figs. 3, 7). A large oxygen emission was seen at station C034 (2522.6 mmol O_2 m^{-2}) close to the eddy center. If this DO emission at station C034 occurred due to the passage of the eddy, an average emission rate of 64.7 mmol O_2 m^{-2} day^{-1} was obtained using the transit time (39 days) of the eddy, which was estimated by the radius of the eddy (200 km) and the transit speed (about 5.1 km day^{-1}). This value corresponds approximately to the net community productivity (NCP) of 45.7 mmol C m^{-2} day^{-1} (548.4 mg C m^{-2} day^{-1}) using the typical elemental ratio of the photosynthesis and remineralization processes (C:N:P:$-O_2$ = 106:16:1:150; Anderson 1995). The largest oxygen emission in this study was observed at station C033 (Table 1), which was passed by three-quarters of the eddy.

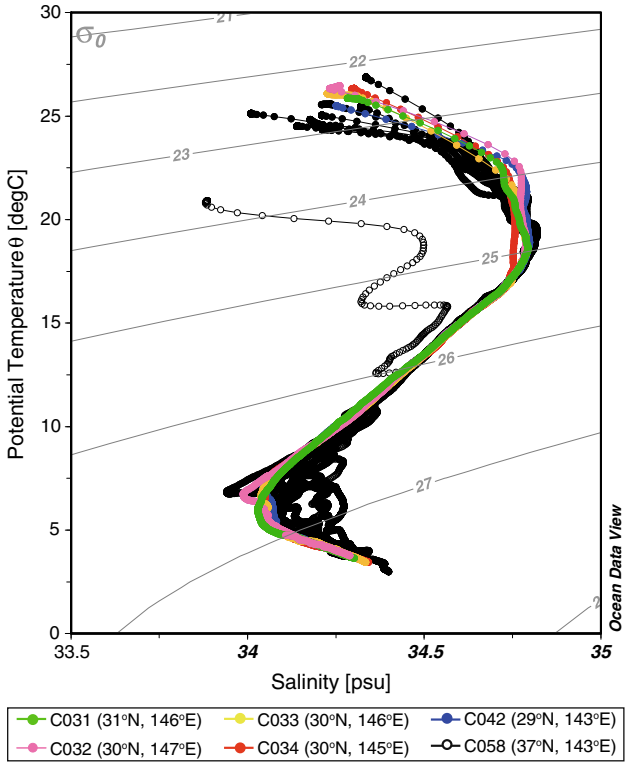

Fig. 8 Temperature–salinity curve for the $CTDO_2$ station. *Colored and black closed dots* and *black lines* indicate the profiles at stations inside and outside the eddy, respectively. *Open dots* and *black lines* indicate stations in the subarctic region

The concentration of nitrate at each density level inside and outside the eddy was estimated in the same way as for DO, but the values for some density levels were linearly interpolated because of the coarser sampling than that used for DO. The largest nitrate supply (216.5 mmol N m^{-2}) was recorded at station C033, which also had the largest oxygen emission (Table 1). The estimated net nitrate supplied by the passage of the eddy was comparable to that reported in a previous study regarding a cyclonic eddy (cyclone *Opal*) in the North Pacific (about 200 mmol N m^{-2}; Mahaffey et al. 2008).

The ratios of O_2 emission to NO_3 supply ($-O_2N$ ratio) varied from 10.5 to 20.2 (Table 1). The $-O_2N$ ratio was larger than the empirical stoichiometric ratio (8.8–10.1; Anderson 1995). The $-O_2N$ ratio in C034 was notably high (20.2). The $-O_2N$ ratios (3.5–5.4) in the layers below the 100 m depth at four stations except C034 were smaller than those (14.1–21.0) in the layers above the 100 m depth. Low $-O_2N$ ratios in the deeper layers resulted from low ratios of O_2 increase to NO_3 decrease. The rate of oxygen consumption by respiration of organisms in the deeper layer would surpass the rate of NO_3 production from organic matter by decomposition and nitrification. The high $-O_2N$ ratio in C034 was derived from the calculation, which only contains the data above the 98 m depth.

5 Conclusion

Our shipboard high-resolution survey in the subtropical region of the western North Pacific revealed the detailed water structure and biological activities in and around a cyclonic eddy. This eddy originated from the meander of the KE at 29°N, 154°E, and propagated westward. A remarkable uplift of the isopycnals from a depth of about 600 m to the seasonal thermocline was observed in the eddy. The inside of the eddy was characterized by high DO and low nitrate concentration in the subsurface layer compared with locations outside the eddy. High DO values in thick SOM layers and deep nitraclines in the eddy suggested that the uplift of isopycnals by the cyclonic eddy induced the injection of nutrients from the disphotic zone, and increased the nutrient uptake and emission of oxygen by phytoplankton. The reduced nitrate in the eddy compared with locations outside was believed to be due to a supply from the deeper layer, which was utilized by phytoplankton as new production in the water column. The average nitrate reduction for five stations in the eddy was 182.0 mmol N m^{-2}. This value was comparable to the nitrate supplied by winter convection in the area where North Pacific subtropical mode water was formed (Sukigara et al. 2011).

The area of formation and the trajectory of the observed cyclonic eddy are important features in the Kuroshio recirculation region (Ebuchi and Hanawa 2001). If this observed eddy supplied nitrate into the euphotic zone over

Table 1 Estimated oxygen emission, nitrate supply, and $-O_2N$ ratio

Station (location)	Range of depth (range of density)	Layer thickness (m)	O_2 emission (mmol m^{-2})	NO_3 supply (mmol m^{-2})	$-O_2N$ ratio
C031 (31N, 146E)	38–158 (23.6–25.2)	121	1994.5	190.1	10.5
C032 (30N, 147E)	46–147 (23.7–25.2)	102	1955.9	169.8	11.5
C033 (30N, 146E)	41–131 (23.3–25.2)	91	2659.3	216.5	12.3
C034 (30N,145E)	40–98 (23.2–25.2)	59	2522.6	124.9	20.2
C042 (29N, 143E)	32–151 (23.2–25.2)	120	2251.0	208.9	10.8

the area where the eddy passed, nitrate at a level of 2.0×10^{11} mol N would be induced into the biogeochemical process in this region. This level was estimated using the nitrate supplied per unit square (about 0.2 mol N m^{-2}) and the area over which the eddy passed [1.0×10^{12} $m^2 = 5.0 \times 10^5$ m (as the eddy diameter) $\times$ 2.0×10^6 m (as the distance that the eddy moved)]. Sasai et al. (2010) reported that during 2002–2006, on average, two cyclonic eddies per year were generated and passed through this area. The process of nutrient supply due to the passage of the cyclonic eddy passage had an important role in the high-stratification season in the oligotrophic subtropical region. To further investigate the detailed impacts of the biogeochemical processes following the passage of an eddy, more interdisciplinary studies, including broad and high-resolution three-dimensional observations around an eddy and a diversified range of sampling parameters, are needed. More meaningful data sets can be obtained by adding even more shipboard observations, intensive observations by autonomous profiling floats with biological (DO, nitrate, and Chl *a*) sensors, long time-series observations using a moored system with a mounted sediment trap and/or biogeochemical sensors, and high-resolution three-dimensional physical–biological models.

Acknowledgments This work was partly supported by Grants-in-Aid for Exploratory Research (no. 17651002) Scientific Research in Priority Areas, "Western Pacific Air-Sea Interaction Study (W-PASS)" from the Ministry of Education, Culture, Sports, Science and Technology; by the Grant-in-Aid for Scientific Research (B) (no. 25287118) from the Japan Society for Promotion of Science (KAKENHI); by the Agriculture, Forestry and Fisheries Research Council (AFFRC) for the study of "Population Outbreak of Marine Life"; by Grants-in-Aid for Creative Scientific Research (no. 17GS0203) from the Ministry of Education, Culture, Sports, Science and Technology and for Scientific Research in Priority Areas "Comprehensive studies of global greenhouse gas cycles in the atmosphere, terrestrial biosphere and oceans". The authors thank the captain, crews, and scientists of the R/V *Hakuho-Maru* of the Japan Agency for Marine-Earth Science and Technology (JAMSTEC). Thanks are also given to members of the Physical Oceanography Group at Tohoku University and members of the laboratory of Satellite Biological Oceanography in Hydrospheric Atmospheric Research Center at Nagoya University for their helpful discussions throughout this study.

References

Anderson LA (1995) On the hydrogen and oxygen content of marine phytoplankton. Deep Sea Res I 42:1675–1680

Armstrong FAJ, Stearns CR, Stickland JDH (1967) The measurement of upwelling and subsequent biological processes by means of the Technicon™ Autoanalyzer™ and associated equipment. Deep Sea Res 14:381–389

Benitez-Nelson CR, Bidigare RR, Dickey TD, Landry MR, Leonard CL, Brown SL, Nencioli F, Rii YM, Maiti K, Becker JW, Bibby TS, Black W, Cai WJ, Carlson CA, Chen F, Kuwahara VS, Mahaffey C, McAndrew PM, Quay PD, Rappé MS, Selph KE, Simmons MP, Yang EJ (2007) Mesoscale eddies drive increased silica export in the subtropical Pacific Ocean. Science 316:1017. doi:10.1126/science.1136221

Benitez-Nelson CR, McGillicuddy DJ (2008) Mesoscale physical–biogeochemical linkages in the open ocean: an introduction to the results of the E-Flux and EDDIES programs. Deep Sea Res II 55:1133–1138

Bibby TS, Gorbunov MY, Wyman KW, Falkowski PG (2008) Photosynthetic community responses to upwelling in mesoscale eddies in the subtropical North Atlantic and Pacific Oceans. Deep Sea Res II 55:1310–1320

Brown SL, Landry MR, Selph KE, Yang EJ, Rii YM, Bidigare RR (2008) Diatoms in the desert: plankton community response to a mesoscale eddy in the subtropical North Pacific. Deep Sea Res II 55:1321–1333

Chelton DB, Schlax MG, Samelson RM (2011) Global observations of nonlinear mesoscale eddies. Prog Oceanogr 91:167–216

Cullen JJ (1982) The deep chlorophyll maximum: comparing vertical profiles of chlorophyll *a*. Can J Fish Aquat Sci 39:791–803

Dickey TD, Nencioli F, Kuwahara VS, Leonard C, Black W, Rii YM, Bidigare RR, Zhang Q (2008) Physical and bio-optical observations of oceanic cyclones west of the island of Hawai'i. Deep Sea Res II 55:1195–1217

Ducet N, Le Traon PY, Reverdin G (2000) Global high-resolution mapping of ocean circulation from TOPEX/Poseidon and ERS-1 and -2. J Geophys Res Oceans 105(C8):19477–19498. doi:10.1029/2000JC900063

Ebuchi N, Hanawa K (2000) Mesoscale eddies observed by TOLEX-ADCP and TOPEX/POSEIDON altimeter in the Kuroshio recirculation region south of Japan. J Oceanogr 56:43–57

Ebuchi N, Hanawa K (2001) Trajectory of mesoscale eddies in the Kuroshio recirculation region. J Oceanogr 57:471–480

Ewart CS, Meyers MK, Wallner ER, McGillicuddy DJ, Carlson CA (2008) Microbial dynamics in cyclonic and anticyclonic mode-water eddies in the northwestern Sargasso Sea. Deep Sea Res II 55:1334–1347

Greenan BJW (2008) Shear and Richardson number in a mode-water eddy. Deep Sea Res II 55:1161–1178

Gruber N, Sarmiento JL (1997) Global patterns of marine nitrogen fixation and denitrification. Glob Biogeochem Cycles 11:235–266

Hayward TM (1994) The shallow oxygen maximum layer and primary production. Deep Sea Res I 41:559–574

Knap A, Jickells T, Pszenny P, Galloway J (1986) Significance of atmospheric-derived fixed nitrogen on productivity of the Sargasso Sea. Nature 320:158–160

Koroleff F (1983) Determination of silicon. In: Glasshoff K, Ehrhardt M, Kremling K (eds) Methods of seawater analysis, 2nd edn. Verlag Chemie, Weinheim, pp 174–183

Lewis MR, Harrison WG, Oakley NS, Hebert D, Platt T (1986) Vertical nitrate flux in the oligotrophic ocean. Science 234:870–873

Mahaffey C, Benitez-Nelson CR, Bidigare RR RR, Rii YM, Karl DM (2008) Nitrogen dynamics within a wind-driven eddy. Deep Sea Res II 55:1398–1411

Martin AP, Pondaven P (2003) On estimates for the vertical nitrate flux due to eddy pumping. J Geophys Res 108(C11). doi:10.1029/2003JC001841

Martin AP, Richards KJ (2001) Mechanisms for vertical nutrient transport within a North Atlantic mesoscale eddy. Deep Sea Res II 48:757–773

McGillicuddy DJ, Robinson AR (1997) Eddy-induced nutrient supply and new production in the Sargasso Sea. Deep Sea Res I 44:1427–1450

McGillicuddy DJ Jr, Robinson AR, Siegel DA, Jannasch HW, Johnson R, Dickey TD, McNeil J, Michaels AF, Knap AH

(1998) Influence of mesoscale eddies on new production in the Sargasso Sea. Nature 394:263–266

McGillicuddy DJ, Anderson LA, Bates NR, Biddy T, Buesseler KO, Carlson CA, Davis CS, Ewart C, Falkowski PG, Goldthwait SA, Hansell DA, Jenkins WJ, Johnson R, Kosnyrev VK, Ledwell JR, Li QP, Siegel DA, Steinberg DK (2007) Eddy/wind interaction stimulate extraordinary mid-ocean plankton blooms. Science 316. doi:10.1126/science.1136256

Michaels AF, Knap AH, Dow RL (1994) Seasonal patterns of ocean biogeochemistry at the U.S. JGOFS Bermuda Atlantic time-series study site. Deep Sea Res I 41:1013–1038

Murphy J, Riley JP (1961) Modified single solution method for the determination of phosphate in natural water. Anal Chem Acta 27:31–36

Nencioli F, Kuwahara VS, Dickey TD, Rii YM, Bidigare RR (2008) Physical dynamics and biological implications of a mesoscale eddy in the lee of Hawai'i: cyclonic *Opal* observations during E-Flux III. Deep Sea Res II 55:1252–1274

Oka E, Toyama K, Suga T (2009) Subduction of North Pacific central mode water associated with subsurface mesoscale eddy. Geophys Res Lett 36:L08607. doi:10.1029/2009GL037540

Oka E, Suga T, Sukigara C, Toyama K, Shimada K, Yoshida J (2011) "Eddy resolving" observation of the North Pacific subtropical mode water. J Phys Oceanogr 41. doi:10.1175/2011JPO4501.1

Oschlies A (2002) Can eddies make ocean deserts bloom? Glob Biogeochem Cycles 16. doi:10.1029/2001GB001830

Sasai Y, Kelvin JR, Ishida A, Sasaki H (2010) Effects of cyclonic mesoscale eddies on the marine ecosystem in the Kuroshio extension region using an eddy-resolving coupled physical–biological model. Ocean Dyn 60:693–704

Shulenberger E, Reid JL (1981) The Pacific shallow oxygen maximum, deep chlorophyll maximum, and primary productivity, reconsidered. Deep Sea Res A 28:901–919

Siegel DA, Peterson P, McGillicuddy DJ Jr, Maritorena S, Nelson NB (2011) Bio-optical footprints created by mesoscale eddies in the Sargasso Sea. Geophys Res Lett 38:L13608. doi:10.1029/2011GL047660

Sukigara C, Suga T, Saino T, Toyama K, Yanagimoto D, Hanawa K, Shikama N (2011) Biogeochemical evidence of large diapycnal diffusivity associated with the subtropical mode water of the North Pacific. J Oceanogr 67:77–85

Weiss RF (1981) Oxygen solubility in seawater. In: UNESCO Technical Papers in Marine Science, No. 36:22